Memoirs of the Faculty of Science, Kyoto University, Series of Physics, Astrophysics, Geophysics and Chemistry, Vol. XXXIII, No. 1. Article 4, 1968.

THE SPOT DIAGRAMS OF SCHMIDT CAMERA

By

Seiichi KAWAI

Division of Applied Physics, Government Industrial Research Institute, Osaka

and

Tomokazu KOGURE

Department of Astronomy, Kyoto University, Kyoto

(*Received October 15, 1968*)

ABSTRACT

The quality of images for some Schmidt cameras, which are designated as Types I~IV and whose design data are given in Table I, is examined with the aid of the spot diagrams. Particular attention is paid on the color aberration over the wide wave-length range $\lambda\lambda$ 3500-8500Å. Following results are obtained in the examinations:

(1) For the cameras with long focal lengths (Cameras of Types I~III), the confusion of images could be reduced within grain size of 20~30 μ when the f-ratio is equal or greater than 3, while it surpasses the grain size when the f-ratio is equal or less than 2.5.

(2) Two corrector plates, at least, are required in order to reduce the color confusion over the above-mentioned wave-length range by changing the corrector plate.

(3) The effect of aperture stop of corrector plate becomes significant when the aperture is stopped down to the neutral zone of corrector plate.

(4) Bowen's method of inserting a plane-parallel plate just before the focal plane is efficient for improving the color confusion over a wide wave-length range, but only in a very limited field around the optical axis.

1. Introduction

Since Bernhard Schmidt introduced the so-called Schmidt camera in 1930, the theory of its aberration has been established through the efforts of Carathéodory[1], Lucy[2], Bowen[3], Linfoot[4], and others.

The optical systems of Schmidt camera is principally composed of a corrector plate and a spherical mirror, and the shape of the former is designed so as to the Seidel aberration is accurately corrected for an particular wave length which we call the basic wave length. For rays of other wave lengths color confusions will inevitably occur owing to the wave-length dependence of the refractive index of corrector-plate glass. It is then a basic problem on the design of optical system to reduce these color confusions within a certain limit over a wide wave-length range.

The purpose of the present investigation is to examine the quality of image

for some Schmidt cameras with the aid of the spot diagrams. Particular attention is paid on the following problems:

1) How many corrector plates, at least, should be prepared in order to reduce the color confusion over a wave-length range from ultraviolet,say λ 3500 Å, to infrared, say λ 8500 Å, by changing the corrector plate?

2) When a corrector plate is once set and it is not exchangeable, are there some ways to reduce the color confusions? The stopping down of the aperture of corrector plate, the shifting of the focal plane for each color, are these effective ways? Or, to what extent can the color confusion be removed by inserting a plane-parallel plate just before the focal plane?

The construction of Schmidt camera which promises achromatic images over a wide wave-length range is a growing requirement in the astronomical observations. It is therefore worthwhile to examine the optical systems of Schmidt camera from this point of view. The present investigation was set about by the proposal of Professor T. Shimizu of Kyoto University for the purpose of obtaining the basic data on the optical system of large Schmidt telescopes which include two largest ones in the world.

The Schmidt cameras submitted to the present investigation count four types, named as Type I, II, III, and IV, whose design data are given in Table I. The Type IV camera is the one now under way of trial production at the Government Industrial Research Institute, Osaka.

Table I. Design data of Schmidt cameras*.

Type	I	II	III	IV
Observatory**	Uppsala	—	Palomer	—
Diameter of corrector plate	1000	1200	1200	400
Diameter of spherical mirror	1780	2100	1830	700
Radius of curvature of spherical mirror	6000	7200	6000	2400
Focal ratio	3	3	2.5	3
Effective field angle	7.5°	7.2°	6.0°	7.0°

* The unit of length is milli-meter.

** The Type I and III cameras correspond to the Schmidt telescopes of the respective observatories only in the diameter of corrector plate and the focal ratio.

2. Preparation for computation

a) Optical system and coordinate system

The optical system is, as shown in Figure 1, composed of a corrector plate, a spherical mirror, and, if necessary, a plane-parallel or spherical filter glass placed just before the focal plane.

The corrector plate has a flat surface on the one side and an aspheric surface which forms a revolution of the fourth order algebraic curve, given by equation (2), on the other side. The latter is faced to the spherical mirror. The vertex of this aspheric surface is also the center of curvature both of the spherical mirror and of the spherical image surface.

The coordinate system is taken here as follows: X-axis coincides with the optical axis directed to the spherical mirror and Y-axis is perpendicular to it. These two axes compose a meridional plane. Z-axis is perpendicular to this

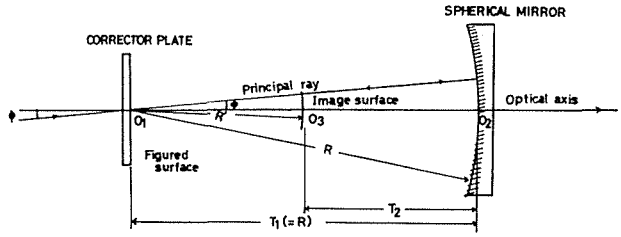

Fig. 1. Optical system.

O_1 : Vertex of the corrector plate, and also the center of curvature both of the spherical mirror and of the image surface.
O_2 : Vertex of the spherical mirror.
O_3 : Vertex of the image surface.
ϕ : Semi-field angle.
R : Radius of curvature of the spherical mirror.
R′ : Radius of curvature of the image surface.
T_1 : Distance between the vertexes of corrector plate and of spherical mirror.
T_2 : Distance between the vertexes of spherical mirror and of image surface.

plane and forms, together with the other axes, a right-handed rectangular coordinate system. The origin of the coordinates is placed at the vertex of corrector plate or of the other surface according to the convenience of computation.

The glass material used for the corrector plate is BK 7. The refractive indices of BK 7 are taken from the data table of Jenaer Glaswerk Schott & Gen., Mainz, except the values at 3500 Å and 8500 Å, for which estimation is made with the aid of the Conrady's interpolation formulae[5] :

$$n=n_0+aw+bw^{3.5}, \tag{1}$$

where

$$n_0=n_d-0.84895(n_f-n_c)+0.92452(n_{g'}-n_f),$$
$$a=0.69108(n_f-n_c)-0.81775(n_{g'}-n_f),$$
$$b=-9.29980(n_f-n_c)+9.63529(n_{g'}-n_f),$$

and $w=1/\lambda$, λ being the wave length of light ray expressed in units of micron. The resultant refractive index is given in Figure 2.

b) Distribution of sampling points

Let us suppose a plane which tangentially contacts with the aspheric surface of corrector plate at its vertex, and make a lattice on this plane with straight lines parallel to Y and Z axes, respectively. The lattice points inside the circle of radius corresponding to the aperture of corrector plate give the sampling points of ray tracing. Each light ray passing through the

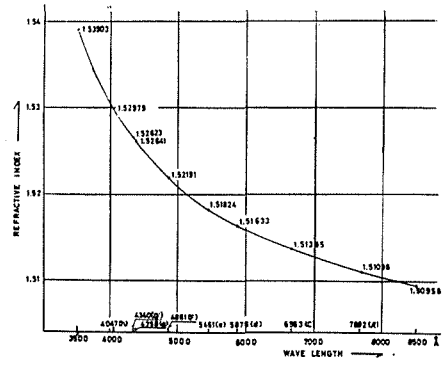

Fig. 2. Refractive index of the glass material BK 7.

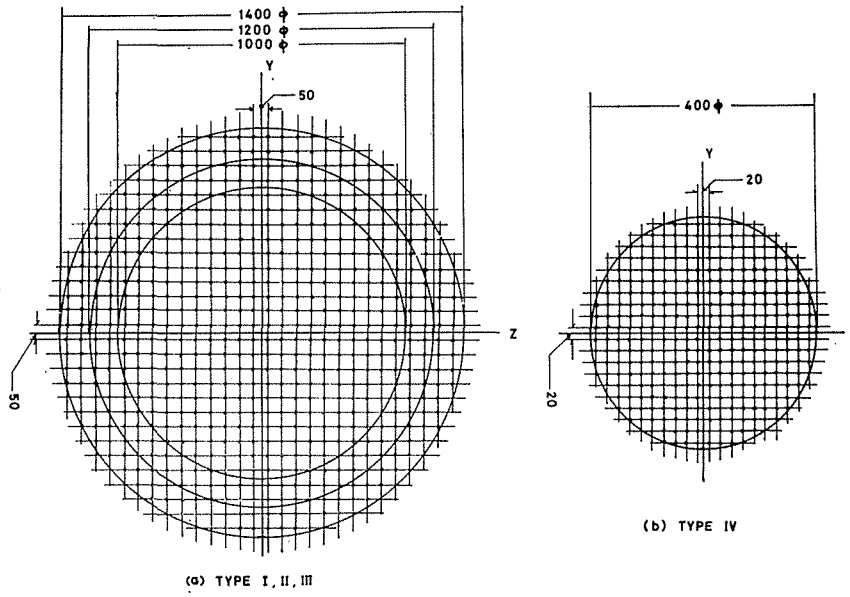

Fig. 3. Distribution of sampling points.

sampling point is reflected at the spherical mirror and transmitted to the image surface to make a spot. The distribution of these spots for parallel incident rays yields a spot diagram of a point light source at infinity.

The light ray passing the vertex of corrector plate in the meridional plane is called the principal ray, which usually makes a semi-field angle ϕ with the optical axis. The ray is called on-axis or off-axis when $\phi=0$ or $\phi\neq 0$, respectively. The sign convention is the same as that of the ordinary ray tracing.

c) Computer

The calculation of ray tracing was carried out with the aid of OKITAC-5090 C at the Government Industrial Research Institute, and the plotting of final data giving the spot diagrams was made by the XYZ-plotter manufactured by Iwasaki Co.

The programming was executed according to the formulae due to Feder[6].

3. Position of best focus

The best focus is, in this paper, defined as the position of the circle of least confusion. This is determined by the following procedure. Since all of the rays reflected at the spherical mirror converges near the best focus, we first put two arbitrary image planes near the converging point and compute the Y coordinates of the points at which the sampling light rays cross these planes. Then, connecting the two corresponding points on these planes, we can find the position of the circle of least confusion, T_2, which is given as the distance from the vertex of the spherical mirror. Examples are shown in Figures 4 and 8.

4. A property on the spherical aberration

The aspheric surface of the corrector plate is expressed by

$$x=\frac{(y^2+z^2)-kD^2(y^2+z^2)^2}{4(n-1)R^3}, \tag{2}$$

where n, R, and D denote the refractive index of corrector-plate glass, radius of curvature of the spherical mirror, and the semi-diameter of corrector plate, repectively. k is an adjustable constant, and Bowen[3] has shown that the chromatic aberration is minimized when $k=1.5$.

According to Bowen[3], the ray passing through the corrector plate at a height y in the meridional plane gives rise to a linear displacement, δ, from the optical axis at the focal plane. In our notation, δ is given by

$$\delta=\frac{(2y^3-kD^2y)}{4R^2}. \tag{3}$$

It is to be noticed that the linear displacement δ is free from the value of n, the index of corrector-plate glass at the basic wave length, in contrast with the shape of aspheric surface of the corrector plate expressed by equation (2). This implies that, once the aperture of corrector plate and the radius of curvature of the spherical mirror are given, the transversal spherical aberration of a ray of the basic wave length is independent of the adopted value of the basic wave length regardless of the shape of corrector plate. The magnitude of aberration is a function only of the incident height at the corrector plate.

This property is confirmed again by the present meridional ray tracing. An example for the transversal spherical aberration in the case of Type IV camera is given in Table II, where the heights of a ray at the corrector plate (incident height), at the main mirror, and at an image plane arbitrarily settled near the best focus, are shown for two basic wave lengths, 5876 Å and 4358 Å. The last column of Table II yields the transversal spherical aberration in question. Agreement is quite satisfactory between two cases of different basic wave lengths for the corresponding incident height. This is the numerical verification of Bowen's property mentioned above.

Table II. Transversal spherical aberration at two different basic wave lengths.

Basic wave length	Position of image plane	Height of ray		
		at corrector plate (incident height)	at spherical mirror	at image place (spherical aberration)
5876Å (d-line)	−1196.8 mm	100.000 mm	99.653076 mm	6.1343607 micron
		150.000	149.80506	8.8675984
		200.000	200.34601	7.5675755
4358Å (g-line)	−1196.8	100.000	99.653074	6.1343607
		150.000	149.80506	8.8675984
		200.000	200.34601	7.5675960

5. Spot diagrams

In this section we present the spot diagrams constructed for various wave lengths and examine the color effect on the quality of images in each type of Schmidt camera given in Table I.

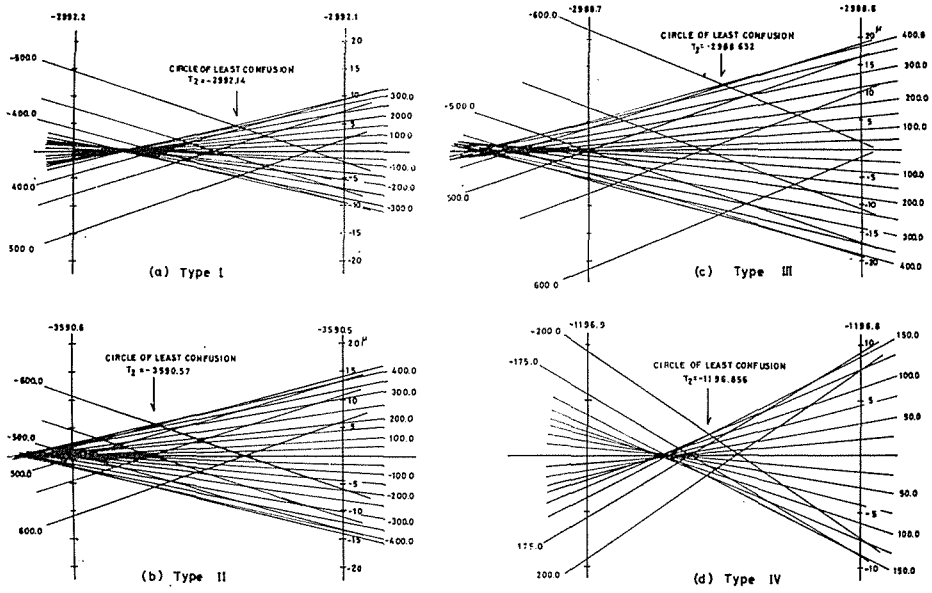

Fig. 4. Convergence of rays near the best focus.
The basic wave length is λ 4358 Å (g-line).

Table III. The best focus and the radius of curvature of image surface.

	The best focus (T_2)	Radius of curvature of image surface (R')
Type I	−2992.14 mm	−3007.86 mm
Type II	−3590.57	−3609.43
Type III	−2988.652	−3011.348
Type IV	−1196.856	−1203.144

Table IV. Diameter of image of on-axis rays. (The basic wave length is λ 4358Å and the unit in length is micron.)

	3500Å	4047Å (h-line)	4358Å (g-line)	4861Å (F-line)	5876Å (d-line)	8500Å
Type I	14.4	5.9	9.5	15.6	24.2	35.2
Type II	17.5	6.6	11.0	18.4	28.6	41.8
Type III	21.4	16.6	23.6	34.0	48.4	66.8
Type IV	5.8	2.3	3.6	6.2	9.7	14.0

Table V. Confusion of image of off-axis rays. (The basic wave length is λ 4358Å and the unit in length is micron.)

	3500Å		g-line		F-line		8500Å	
	$Y_{max}-Y_{min}$	$Z_{max}-Z_{min}$	$Y_{max}-Y_{min}$	$Z_{max}-Z_{min}$	$Y_{max}-Y_{min}$	$Z_{max}-Z_{min}$	$Y_{max}-Y_{min}$	$Z_{max}-Z_{min}$
Type I	28.3	15.8	14.8	8.8	16.8	14.5	32.8	34.0
Type II	31.1	19.0	15.6	10.1	19.0	17.3	39.4	39.8
Type III	33.1	22.6	26.3	22.8	34.4	33.0	64.7	65.6
Type IV	10.3	6.2	5.4	3.5	6.5	5.9	13.3	13.7

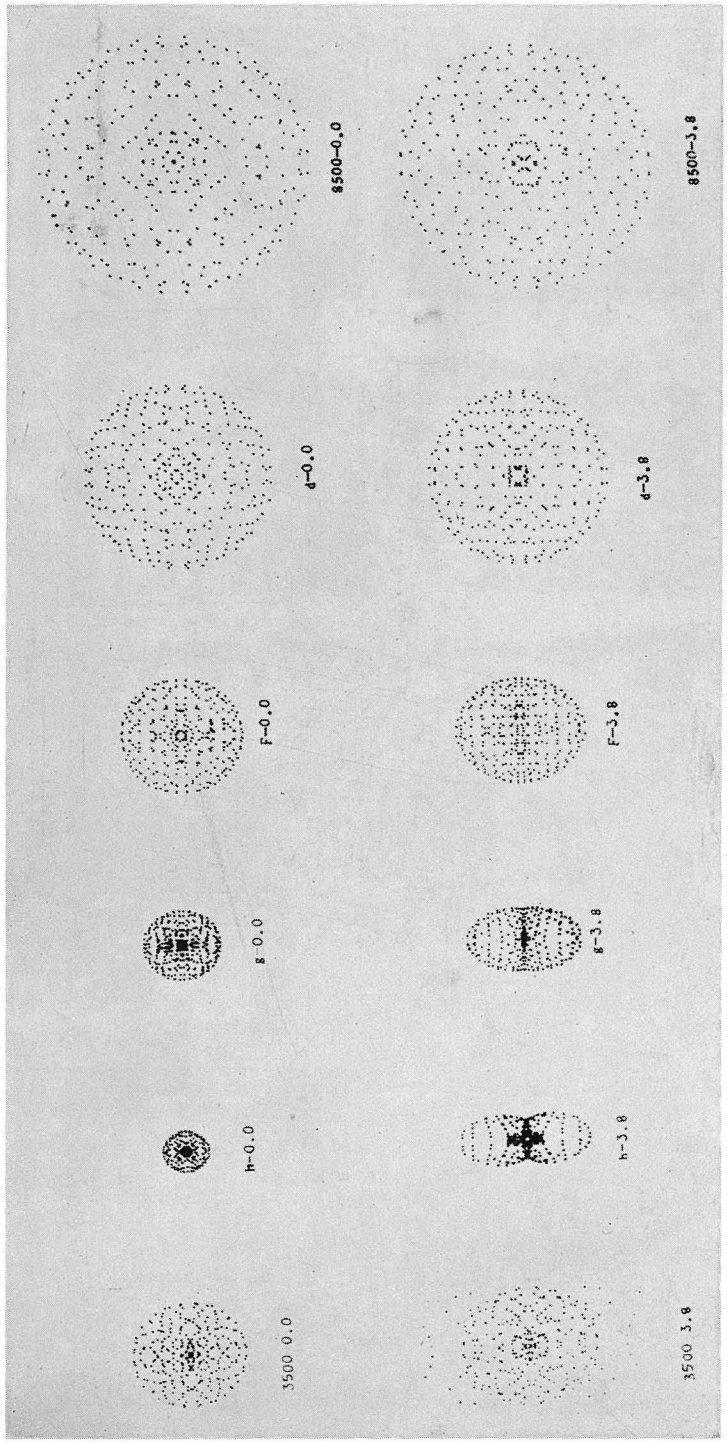

Fig. 5a. Spot diagrams of Type I camera at the position of best focus. The basic wave length is λ 4358Å. The upper and lower parts correspond to the cases of on-axis ray (ϕ=0.0°) and of off-axis ray (ϕ=3.8°), respectively.

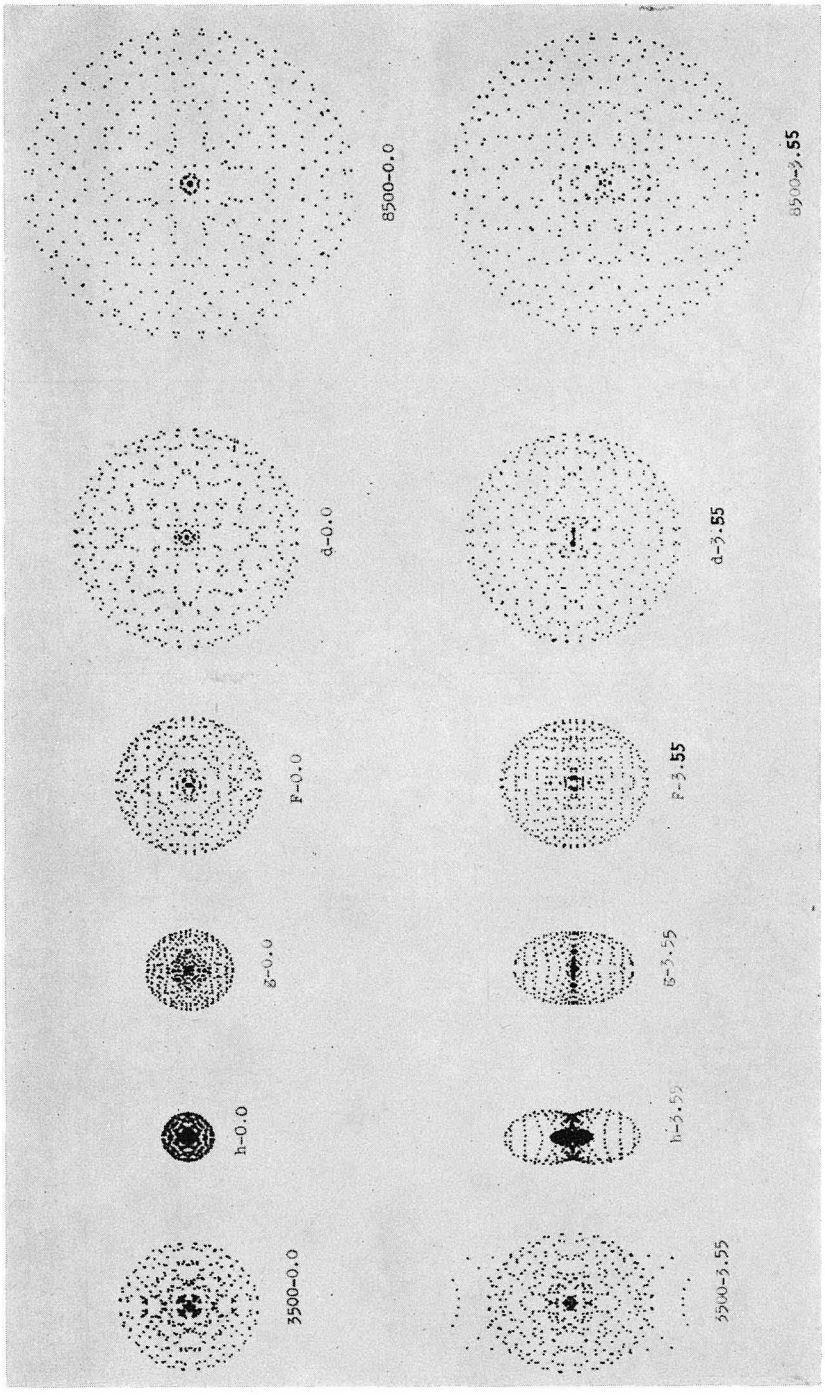

Fig. 5b. Spot diagrams of Type II camera. Explanation is the same as in Figure 5a except the value of $\phi=3.55^\circ$ for the off-axis ray.

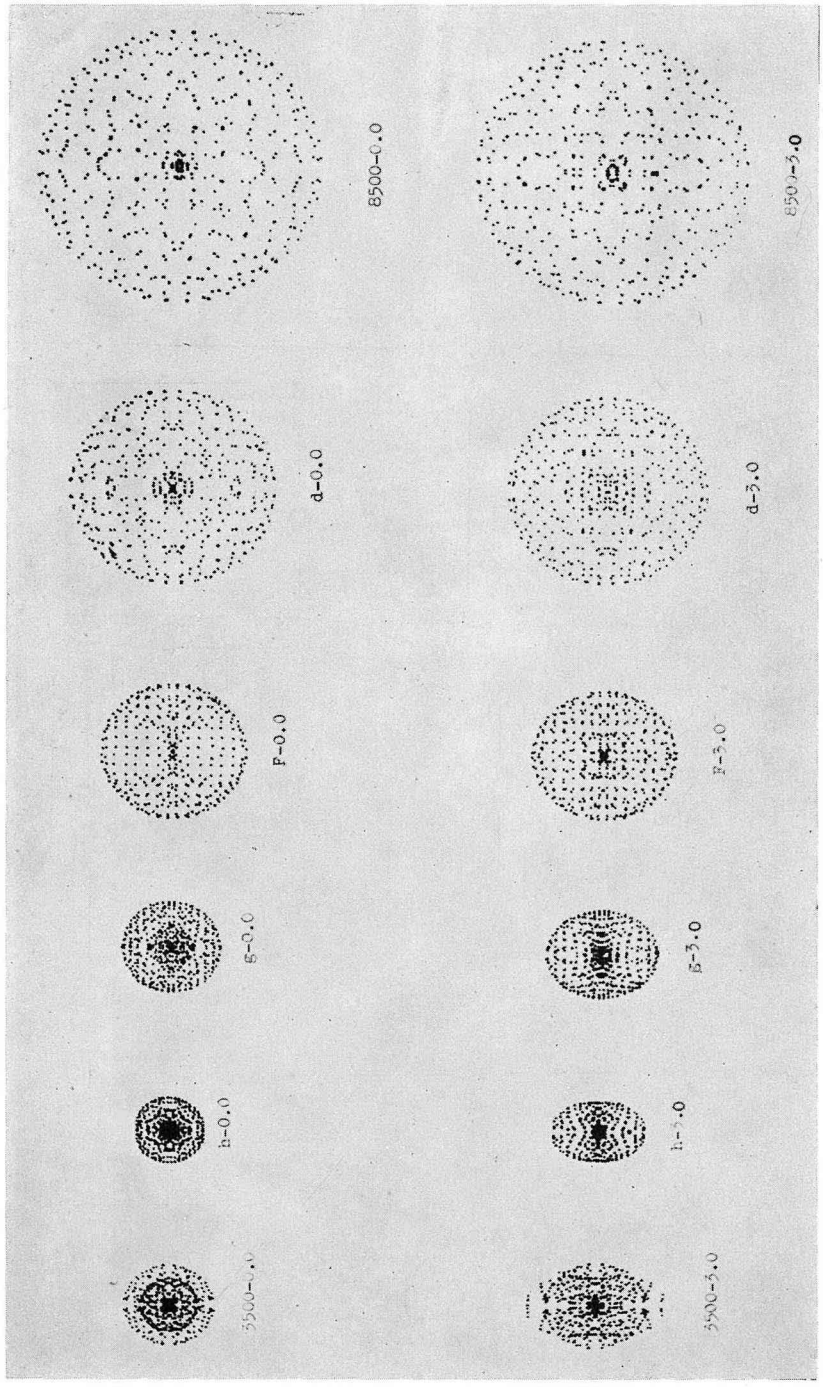

Fig. 5c. Spot diagrams of Type III camera. Explanation is the same as in Figure 5b except the value of $\phi=3.0°$ for the off-axis ray.

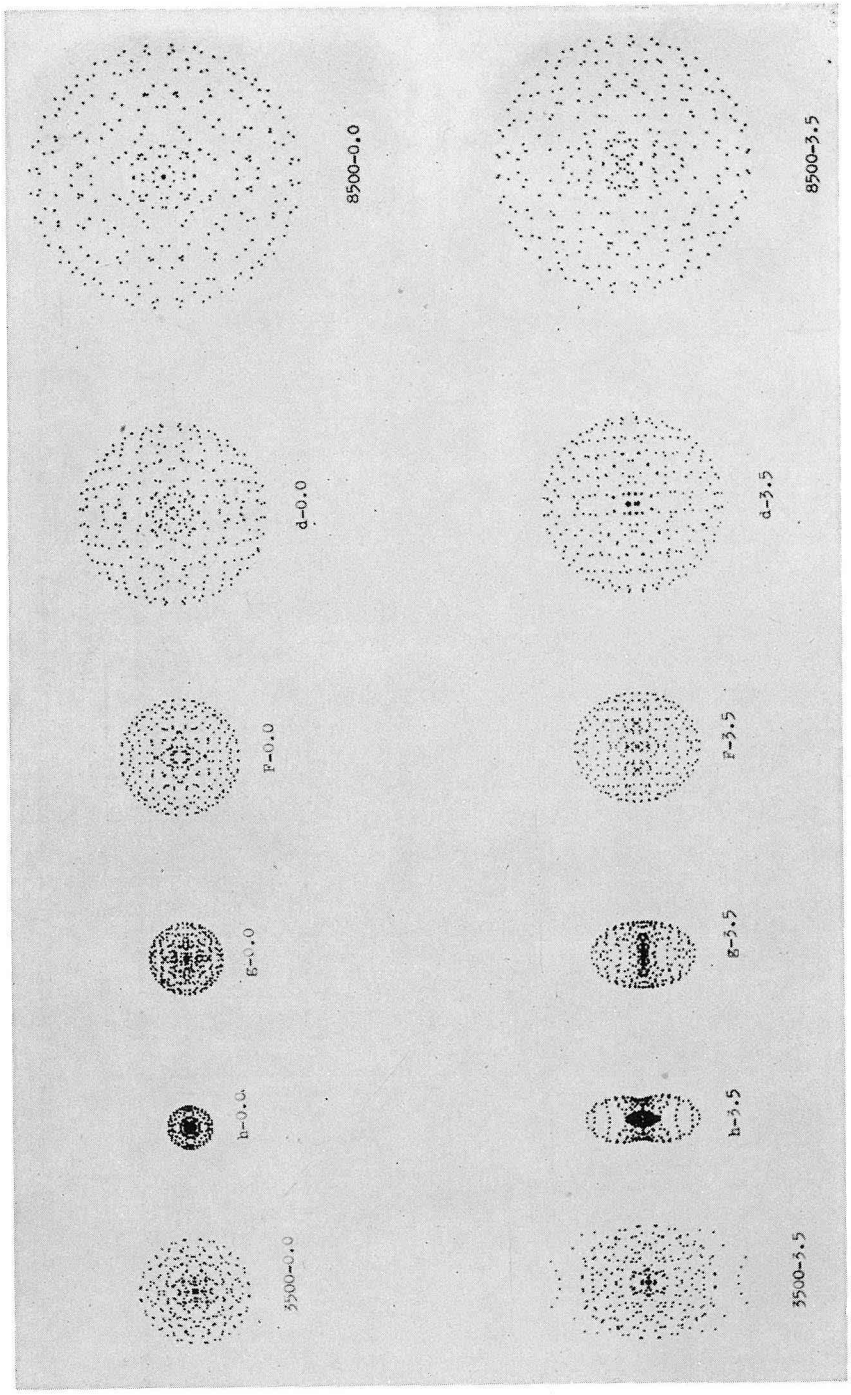

Fig. 5d. Spot diagrams of Type IV camera. Explanation is the same as in Figure 5a except the value of $\phi=3.5°$ for the off-axis ray.

The first series of Figures gives the cases in which the basic wave length of λ 4358 Å (g-line) is used for determining the shape of corrector plate. Figures 4a~4d illustrate the convergence of rays near the best focus for the cameras of Types I~IV, respectively. The position of best focus and the radius of image surface are shown in Table III. In Figures 5a~5d are shown the spot diagrams at six wave lengths computed at the best focal surface of basic wave length. The upper half of each figure yields the case of on-axis ray and the lower half the case of off-axis ray. The diameter of images of on-axis ray and the confusion of images of off-axis ray are summarized in Tables IV and V.

The second series of Figures is devoted to the cases of the basic wave length λ 6563 Å (C-line). Figure 6 shows the convergence of rays near the best focus for the Type IV camera. When compared with Figure 4d, the agreement between these two figures is quite satisfactory, regardless of difference in the adopted basic wave length. This is an another verification of the property stated in Section 4. Spot diagrams at six wave lengths are shown in Figures 7a~7d. The image sizes in these cases are given in Tables VI and VII, for on-axis and off-axis rays, respectively

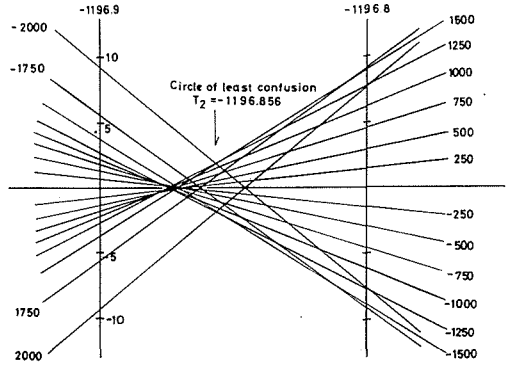

Fig. 6. Convergence of rays near the best focus for Type IV camera. The basic wave length is λ 6563 Å (C-line).

Table VI. Diameter of image of on-axis rays. (The basic wave length is λ 6563Å and the unit in length is micron.)

	3500Å	4861Å (F-line)	6563Å (C-line)	7682Å (A'-line)	8500Å
Type I	35.8	7.6	9.5	13.6	15.6
Type II	43.0	9.3	11.0	16.0	18.6
Type III	57.0	11.8	23.8	30.6	34.2
Type IV	14.2	3.0	3.8	5.4	6.2

Table VII. Confusion of image of off-axis rays. (The basic wave length is λ 6563Å and the unit in length is micron.)

	3500Å		4861Å (F-line)		6563Å (C-line)		8500Å	
	$Y_{max}-Y_{min}$	$Z_{max}-Z_{min}$	$Y_{max}-Y_{min}$	$Z_{max}-Z_{min}$	$Y_{max}-Y_{min}$	$Z_{max}-Z_{min}$	$Y_{max}-Y_{min}$	$Z_{max}-Z_{min}$
Type I	45.9	36.8	22.3	9.4	14.8	8.8	17.3	14.8
Type II	52.1	44.4	23.9	10.6	15.7	10.1	19.1	17.4
Type III	63.3	58.0	24.0	12.6	26.4	22.6	34.6	33.0
Type IV	16.5	14.6	7.8	3.4	5.4	3.5	6.5	5.9

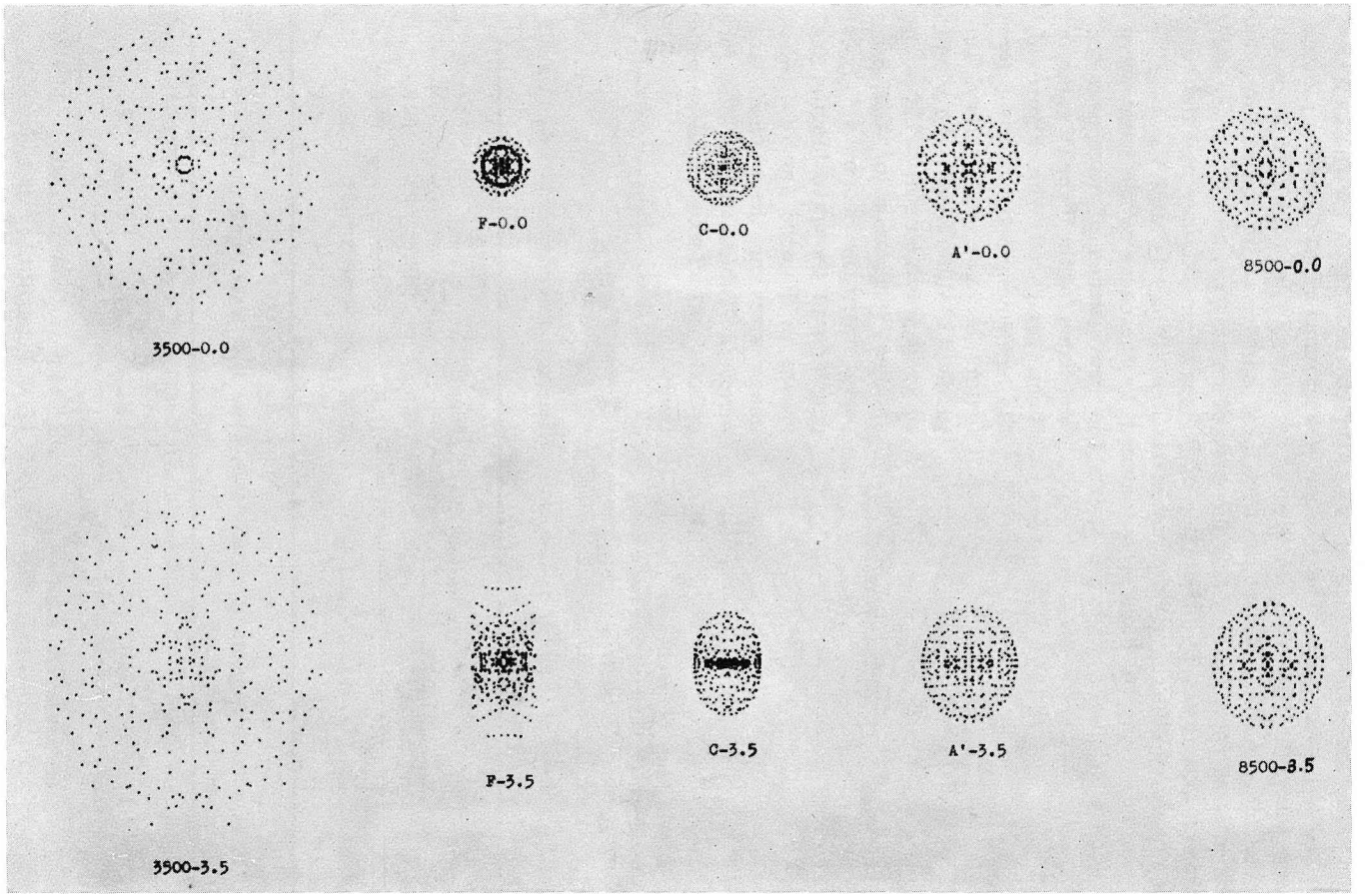

Fig. 7a. Spot diagrams of Type I camera at the position of best focus. The basic wave length is λ 6563 Å. The upper and lower parts correspond to the cases of on-axis ray (ϕ=0.0°) and of off-axis ray (ϕ=3.8°), respectively.

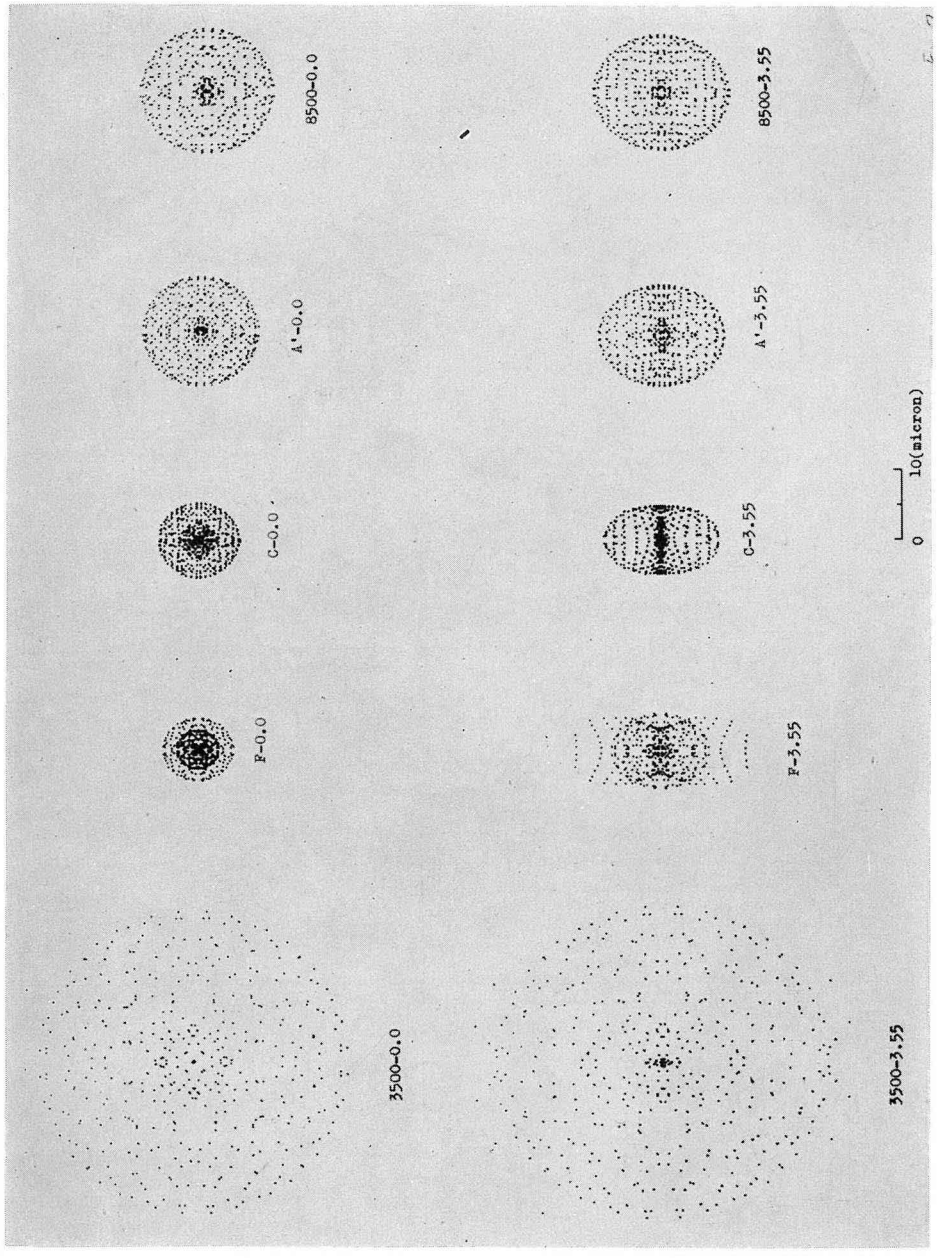

Fig. 7b. Spot diagrams of Type II camera. Explanation is the same as in Figure 7a except the value of $\phi=3.55°$ for the off-axis ray.

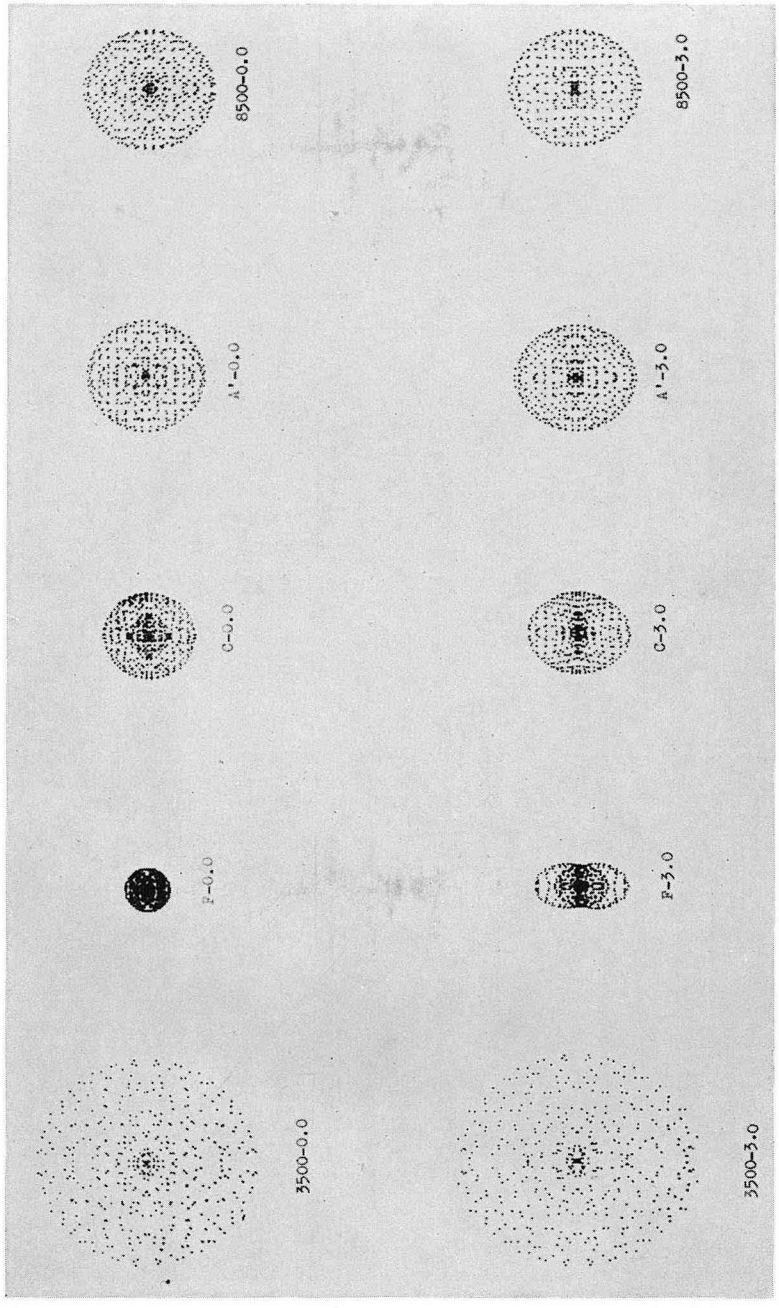

Fig. 7c. Spot diagrams of Type III camera. Explanation is the same as in Figure 7a except the value of $\phi=3.0°$ for the off-axis ray.

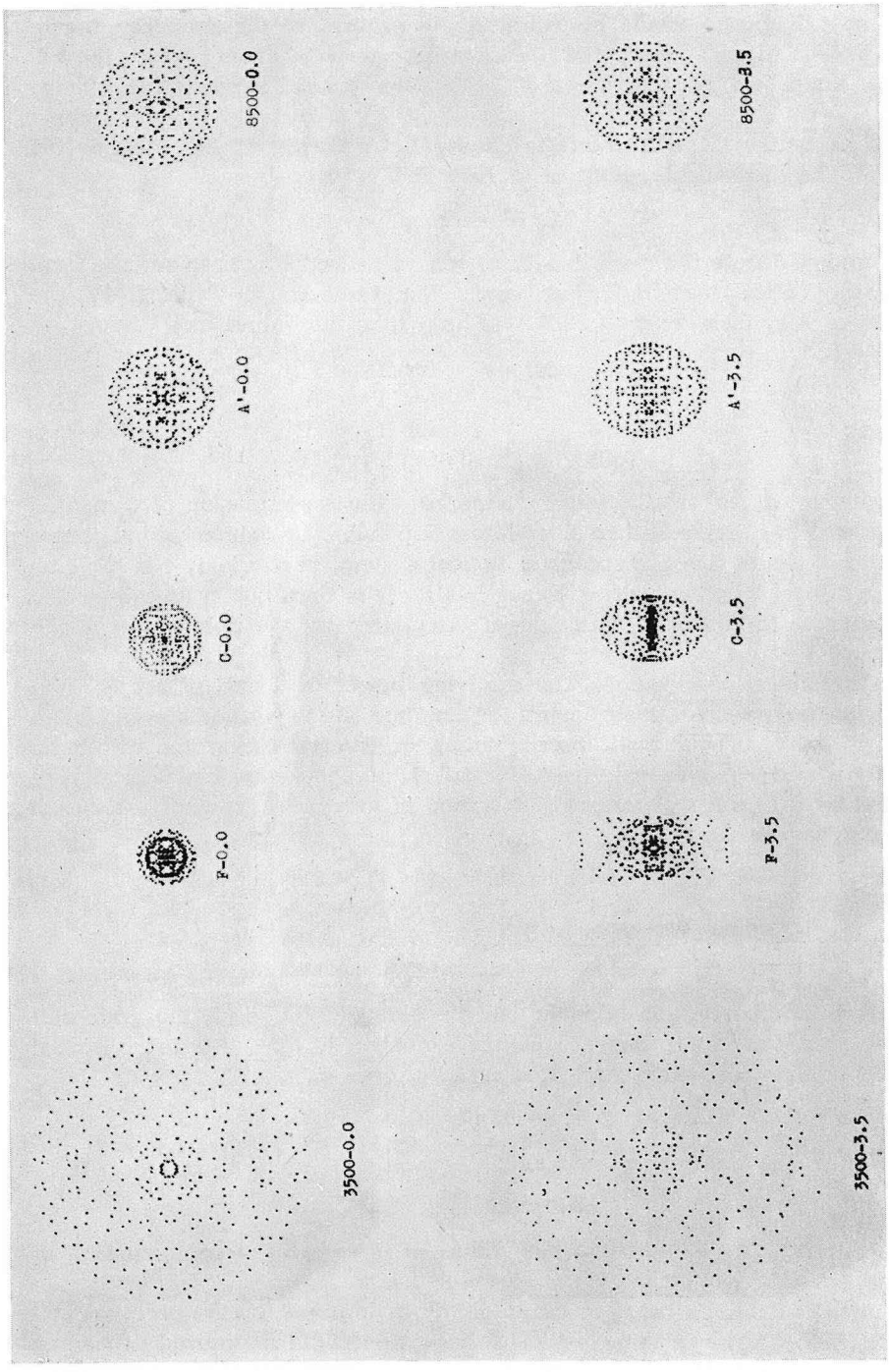

Fig. 7d. Spot diagrams of Type IV camera. Explanation is the same as in Figure 7a except the value of $\phi=3.5^{\circ}$ for the off-axis ray.

6. Examination of the spot diagrams

The spot diagrams should be examined, in general, by the extension, homogeneity, and/or the asymmetry of the distributing spots, among which the extension of image should be compared with some critical length on the image surface.

Ideally speaking, it is desirable to employ the diameter of Airy disk as the criterion. The theoretical radius, ρ, of Airy disk is given by

$$\rho = 1.22\,\lambda F \text{ microns},$$

where λ and F denote the wave length of ray measured in micron and the focal ratio of the optical system, respectively. For cameras of Types I~IV, the diameters of Airy disk, 2ρ, at λ 5876 Å (d-line) take the values as

$$2\rho = \begin{cases} 4.3 \text{ microns} & \text{for Type I} \\ 4.3 & \text{for Type II} \\ 3.8 & \text{for Type III} \\ 4.3 & \text{for Type IV} \end{cases}$$

These values are so small, when compared with the extension of computed spot diagrams in Section 5, that it is almost impossible to reduce the image size within these values by any realistic optical system, particularly for cameras with longer focal lengths such as Types I~III. It is then not practical for the present purpose to adopt the diameter of Airy disk as the criterion of image inspection.

In astronomical observations, the resolving power of 1 sec. of arc is often required for the precise measurement, for example, in the position determination of stars, in the morphological discrimination of faint galaxies, and in others. On the focal surface, this scale length is called the photographic plate scale and designated by q in units of micron per second of arc. The value of q for each camera is given as

$$q = \begin{cases} 14.5 \text{ microns} & \text{for Type I} \\ 17.4 & \text{for Type II} \\ 14.5 & \text{for Type III} \\ 5.8 & \text{for Type IV} \end{cases}$$

Moreover, when observation is made on the photographic plate, the grain size also limits the quality of image. In the emulsion of ordinary astronomical photographic plate, the grain size, p, is usually given as

$$p = 20 \sim 30 \text{ microns}.$$

In this way we have a general relation:

$$p > q \quad \text{and} \quad q > 2\rho.$$

This infers that one may adopt the value of p as the practical criterion of image inspection.

Let us now examine the spot diagrams by making use of the practical criterion, p. Since, however, the result of inspection could be altered depending on which value of p, $p=20$ or $p=30$, is used, we shall make our inspection for these two values, separately. The preference of the value of p properly depends

on the purpose of observations.

Once the value of p is given, the achromatic range for each optical system is defined as the spectral region within which the extension of image is always smaller than p.

(1) Case of $p=20\,\mu$

The achromatic range may be determined from Tables IV, V, and Figures 5a~5d when the basic wave length is λ 4358 Å (g-line), or, from Tables VI, VII, and Figures 7a~7d when the basic wave length is λ 6563 Å (C-line). The results are as follows:

	Achromatic range ($p=20\mu$)	
Basic wave length	4358Å	6563Å
Types I and II	3500-4861Å	4861-8500Å
Type III	Not exist	Not exist
Type IV	Whole spectral region (3500-8500Å)	

In deriving these achromatic ranges, allowance is made in estimating the size of elongated image of off-axis ray as a circle of its minor axis. This is by the reason that the distribution density of dispersed spots is so low that these spots scarecely contribute to actual image formation in the practical photography.

(2) Case of $p=30\,\mu$

The same tables and figures as in the above case yield the following achromatic ranges under the same allowance for elongated images of off-axis rays.

	Achromatic range ($p=30\mu$)	
Basic wave length	4358Å	6563Å
Types I and II	3500-5876Å	4861-8500Å
Type III	3500-4358	4861-7682
Type IV	Whole spectral region (3500-8500Å)	

It is shown as the result that, for Schmidt cameras of long focal lengths such as Types I~III, the focal ratio 3 is a critical value in the examination of images. For cameras of Types I and II with 3.0/F, the achromatic range is able to cover the whole spectral region of $\lambda\lambda$ 3500-8500 Å even in the case of $p=20\,\mu$, if the two corrector plates, one of which is designed for the wave length λ 4358 Å and the other is for λ 6563 Å, are prepared as exchangeable. On the other hand, the confusion of image of Type III camera with 2.5/F could not be reduced to within $p=20\,\mu$ at any wavelength. Only under the lenient criterion of $p=30\,\mu$, the achromatic range could cover the main part of the above spectral region. Besides, the small Schmidt camera such as Type IV provides the achromatic images over the whole spectral region by a single corrector plate when it is prepared at a suitable wave length.

7. Effect of aperture stop of corrector plate

Let us define in advance the neutral zone of corrector plate as the height in Y-axis at which tangential plane to the aspheric surface is parallel to YZ-plane. Usually the neutral zone appears at about 80 percent of the full aperture.

Now, from the examination of Figures 4(c) and 8 on the Type III camera, we easily ascertain the two properties concerning the color confusion of images: (i) the large confusions of image at the lines of g (the basic wave length), d, A', and at λ 8500 Å are mainly attributed to the marginal rays which are incident upon the corrector plate outside the neutral zone (D=519.6 mm for Type III camera), and (ii) the position of best focus at each color remains almost unchanged within the limit of 0.01 mm in its displacement.

The second property infers that the adjustment of the position of focal plane has negligent effect on reducing the color confusion. That is to say, the spot diagrams given in Figure 5c, which are constructed on the image surface of the basic wave length λ 4358 Å, will not be improved even after the image surface is shifted to the respective position asigned in Figure 8.

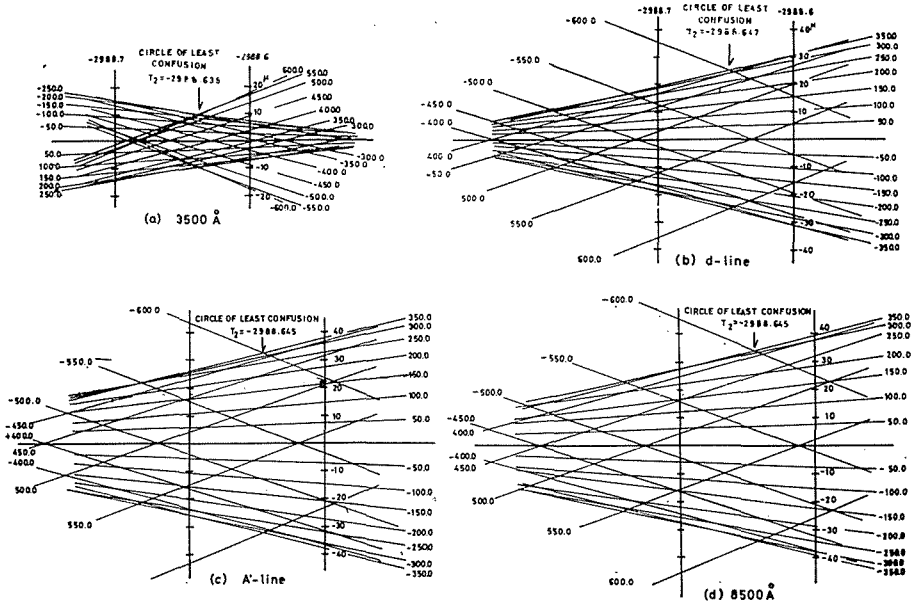

Fig. 8. Convergence of rays in Type III camera for various wave lengths. The basic wave length is λ 4358 Å.

On the contrary, the property (i) provides a possibility of reducing the color confusion, if the aperture stop of corrector plate and the adjustment of focal surface are both permissible. In order to investigate this effect on the case of Type III camera, let us consider the modified camera, designated as Type III′, whose aperture of corrector plate is stopped down to its neutral zone. After determining the position of best focus by the meridional ray tracing, the spot diagrams at five wave lengths are constructed and shown in Figure 9. One

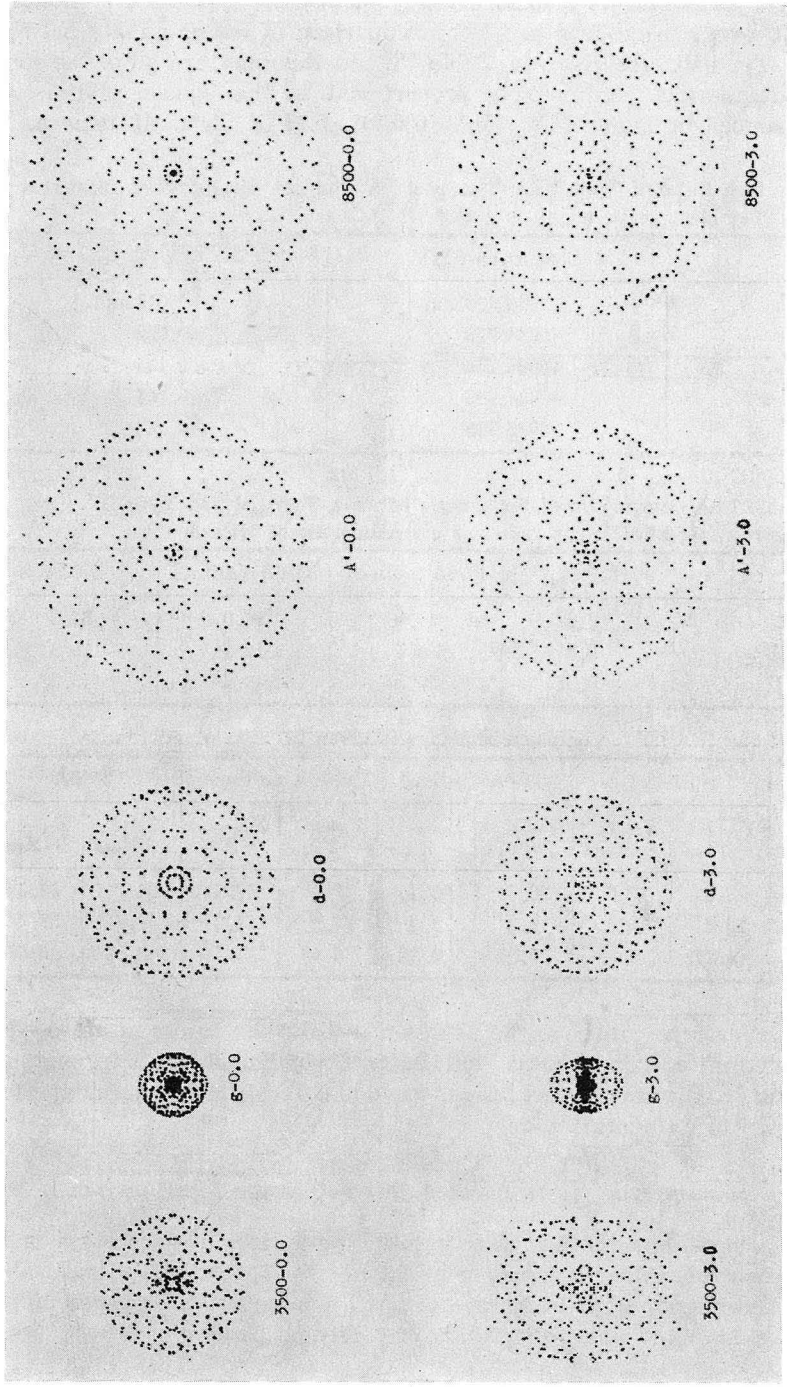

Fig. 9. Spot diagrams of Type III camera indicating the effect of aperture stop of corrector plate at various wave lengths. The corrector plate is stopped down to the neutral point and the basic wave length is λ 4358 Å. The upper and lower parts correspond to the on-axis ray (ϕ=0.0°) and off-axis ray (ϕ=3.0°), respectively.

imediately sees that the quality of image is considerably improved: the color confusion is reduced and the unsymmetric aberration does not appear. The position of best focus and its displacement from that of Type III are shown in Table VIII at every wave-length. The comparison of image quality between Type III and Type III′ are given in Table IX. In this aperture stop, the speed of optical system, which is inversely proportional to the square of the focal ratio, F, is reduced in Type III′ to $(519.6/600.0)^2=0.75$ of Type III camera.

Table VIII. Best focus of Type III′. The position and its displacement from that of Type III. (The basic wave length is λ 4358Å.)

	Best focus (T_2)	Displacement of best focus T_2(III′)$-T_2$(III)
3500Å	−2988.633 mm	+0.019 mm
g-line	−2988.710	−0.058
d-line	−2988.756	−0.104
A′-line	−2988.786	−0.134
8500Å	−2988.793	−0.141

Table IX. Comparison of the images between Type III and Type III′.

(a) On-axis ray ($\phi=0.0$): Image radius is given in units of micron.

	3500Å	4358Å (*g*-line)	5876Å (*d*-line)	8500Å
Type III	9.6	11.9	25.0	34.2
Type III′	9.3	4.1	12.2	18.8
(III′)/(III)	0.97	0.34	0.49	0.55

(b) Off-axis ray ($\phi=3.0°$): Confusion of image is given in units of micron.

	3500Å		4358Å (*g*-line)		5876Å (*d*-line)		8500Å	
	$Y_{max}-Y_{min}$	$Z_{max}-Z_{min}$	$Y_{max}-Y_{min}$	$Z_{max}-Z_{min}$	$Y_{max}-Y_{min}$	$Z_{max}-Z_{min}$	$Y_{max}-Y_{min}$	$Z_{max}-Z_{min}$
Type III	33.0	22.6	26.3	23.0	47.4	47.2	64.7	65.6
Type III′	25.4	18.8	9.3	8.0	22.7	24.0	33.7	37.4
(III′)/(III)	0.77	0.83	0.35	0.35	0.48	0.51	0.52	0.57

For any other type cameras, the situation will be the same, and the effect of aperture stop of corrector plate will become significant for improving the color confusion, particulary in the longer wave-length region, when the aperture is stopped down to its neutral zone.

8. Effect of a plane-parallel plate inserted just before the focal surface

Bowen[3] pointed out that a plane-parallel plate which was placed in the converging beam introduced a small amount of over-corrected spherical aberration. He then suggested to make use of such a plate for the purpose of correcting the residual chromatic aberration of corrector plate over a wide wave-length range.

Let n and n' be the refractive indices of corrector-plate glass at the basic

wave length, which is suitably chosen near the short wave-length end of color range, and at the wave length in question, respectively, and also, let N be the refractive index of the plane-parallel plate at the wave length in question. Then the thickness of the plane-parallel plate, d', which assures the required correction of color confusion, is given by, after Bowen,

$$d' = \frac{N^3 f(n-n')}{4(N^2-1)(n-1)}. \tag{4}$$

On the basis of this formula let us examine the effect of the plane parallel plate in the case of Type I camera. The disposition of optical elements is shown in Figure 10, together with the necessary symbols of geometrical relations which are designated similarly with those of Figure 1. In Figure 10 the symbols T_3, R_2 and R_3 denote the thickness and radii of curvature of both sides of the inserted plate, and T_4 indicates the distance between the image surface and the inserted plate on the X-axis. In the present case we put $T_3=d'$, $R_2=R_3=\infty$, and $T_4=0.0$. We shall call this modified camera as Type I′.

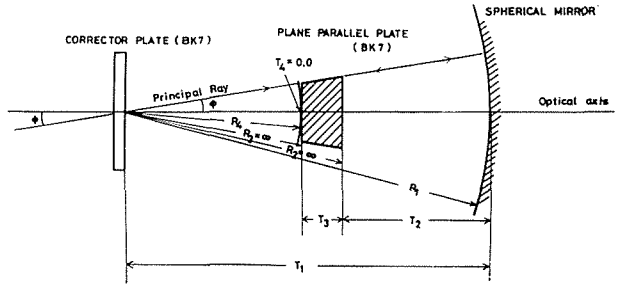

Fig. 10. Disposition of optical system when a plane-parallel plate is inserted just before the image surface.

The basic wave length adopted here is λ 3500 Å and the design data of Type I′ camera are given in Table X. The spot diagrams computed for the basic wave length λ 3500 Å are illustrated in Figure 11. The upper two diagrams are of Type I camera for the cases of on-axis and of off-axis of $\phi=3.8°$ at their best focal surfaces. The middle three are the spot diagrams of Type I′ camera for the on-axis rays at the wave lengths $\lambda\lambda$ 4047, 5876, and 8500 Å, respectively, while the lower three are the same diagrams for the off-axis rays of $\phi=3.8°$.

It is remarkable in Figure 11 that, in the case of on-axis ray of Type I′ camera, the image quality is excellently improved over the whole wave-length

Table X. Design data of Type I′ at three wave lengths for the basic wave length λ 3500Å. (The refractive indices appeared in equation (4) are: $n=1.53903$ at 3500Å and $n'=N$ at the other wave lengths).

	$n'=N$	T_2	$T_3(=d')$	T_4	R_2	R_3	R_4
4047Å (h-line)	1.52979	−2969.926 mm	− 34.2 mm	0.0	∞	∞	−2995.874 mm
5876 (d-line)	1.51633	−2937.008	− 84.1	0.0	∞	∞	−2978.892
8500	1.50958	−2920.296	−109.1	0.0	∞	∞	−2970.604

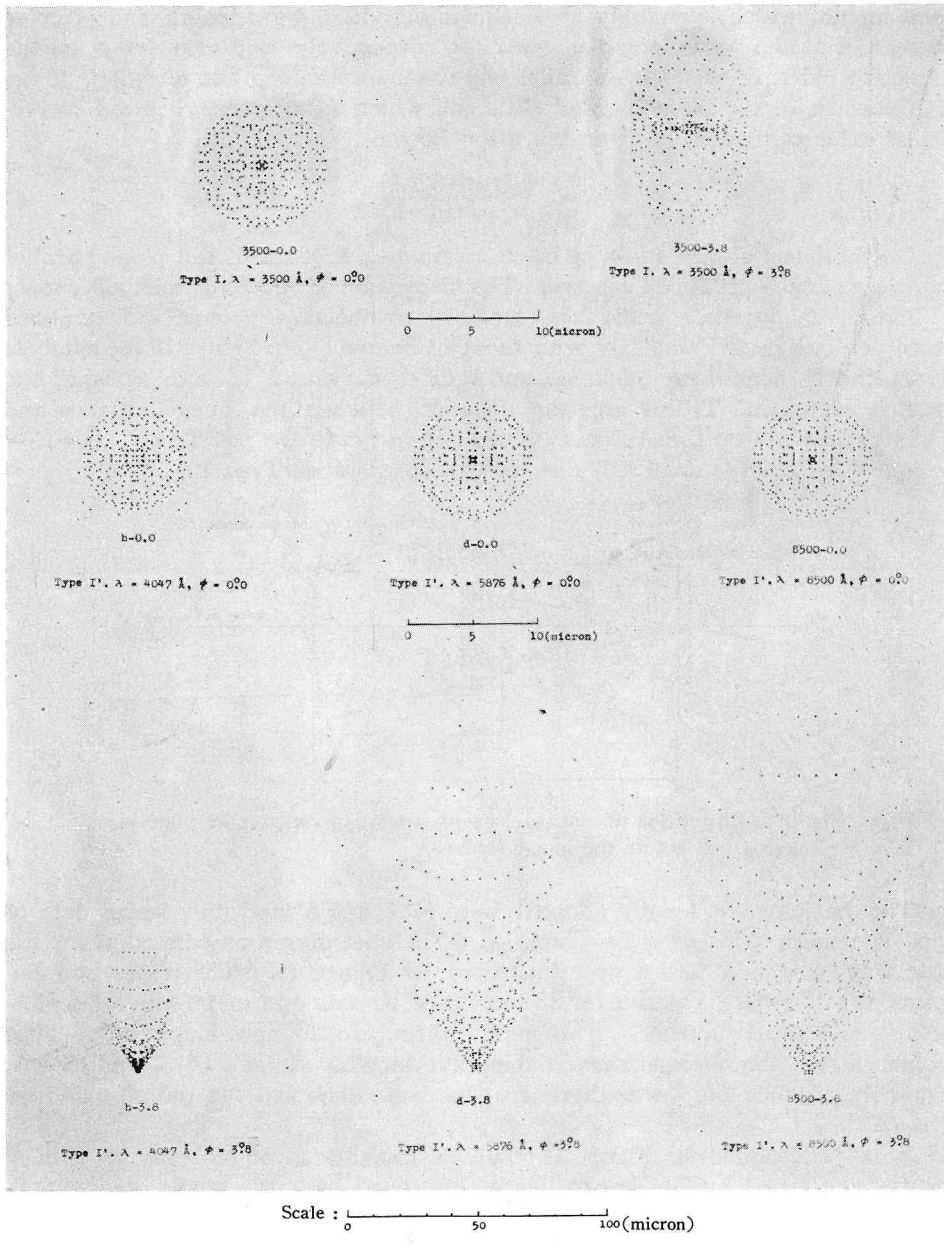

Fig. 11. Spot diagrams of Type I and Type I′ cameras for illustrating the effect of plane-parallel plate inserted just before the focal surface. The basic wave length is λ 3500 Å.

range from 3500 Å to 8500 Å. On the contrary, in the case of off-axis ray, there appears asymmetric off-axis aberration (coma) in each color and the confusion of image increases even up to 150 microns at λ 8500 Å. These results infer that the effect of a plane-parallel plate in the improvement of color confusion

over a wide wave-length range is excellent but only in a very limited semi-field angle. Moreover, one must bear in mind that the thickness of the plane-parallel plate increases with increasing of wave length as seen from Table X and it reaches even 10 cm at λ 8500 A.

9. Effect of extended aperture of corrector plate

In the preceding sections, it has become evident, for the Schmidt cameras with long focal lengths such as Types 1~III, that the confusion of image can be reduced within the grain size of $p=20$ or $30\,\mu$ only when the f-ratio is equal to or larger than 3. Sometimes, however, there arises a strong requirement for a high-speed camera with the f-ratio of 2.5 or less, even at some sacrifice of image quality. For example, photometric observations of faint extended nebulosities will be favored by such a camera.

As already seen, Type II camera principally serves for high-resolution ob-

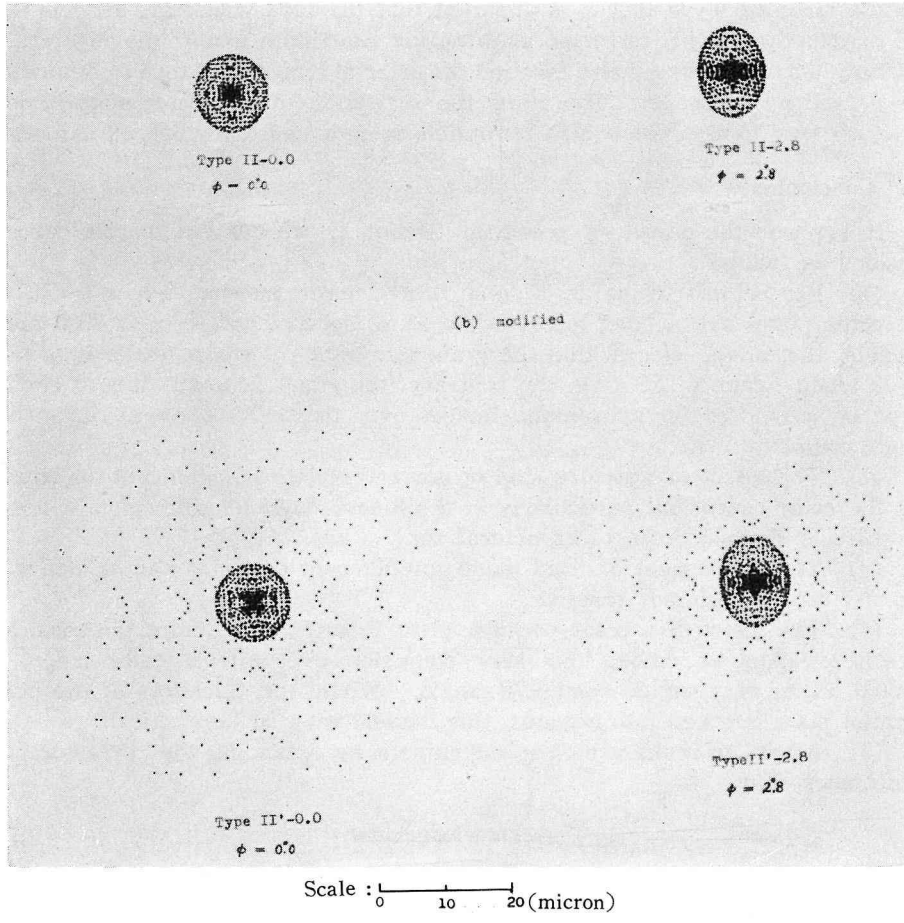

Fig. 12. Spot diagrams of Type II camera for showing the effect of aperture extension. The apertures of Types II and II′ are 1200 mm and 1400 mm respectively. The basic wave length is λ 5876 Å.

servations by its image of high quality. If the corrector plate is set extensible over the normal aperture of Type II camera and other part of the optical system is left as it is, then we shall have a high-speed camera according to observer's requirement. Usually one may stop the corrector plate down to its normal aperture. By this way of aperture extension, can we reconcile the two requirement of high-resolution observations and of a high-speed camera? In order to investigate this problem we examine the image quality of this modified camera which we call Type II′. The optical system of Type II′ camera differs from that of Type II in the following points: the semi-diameter of corrector plate is 700.0 mm where the extension is made as an extrapolation of equation (2) for the original semi-diameter of 600.0 mm, the focal ratio is 2.6 and the unvignetted semi-field angle is 2.8°.

In Figure 12 are shown the spot diagrams, computed at the best focus of of Type II for the basic wave-length λ 5876 A (d-line). Figure 12(a) gives the spot diagrams for the original Type II camera, and Figure 12(b) gives those for the modified Type II′. It is apparent that the rays which are incident upon the extended zone of corrector plate do not contribute to the image formation but only act to produce halos arround the original images and thus to deteriorate the definition of image. Therefore the extension of corrector plate is not a practical way to combine a high-resolution camera and a high-speed camera.

10. Conclusion

In reply to the questions posed in Section 1, we can summarize our conclusions as follows:

(1) For Schmidt cameras of long focal lengths such as Types I~III, two corrector plates are needed to cover the whole spectral range of $\lambda\lambda$ 3500-8500 A keeping the image size within the grain size of $p=20$ when f-ratio is 3, or of $p=30$ when f-ratio is 2.5. On the contrary, the small Schmidt camera such as Type IV provides the achromatic images over the whole spectral region by a single corrector plate.

(2) The effect of aperture stop of corrector plate is significant for improving the color confusion, particularly in the longer wave-length region, when the aperture is stopped down to its neutral zone.

(3) The adjustment of focal plane for different colors is almost ineffective for any type of Schmidt cameras.

(4) The effect of a plane-parallel plate inserted just before the focal surface is excellent to remove the color confusion over a wide color range, but limited in a very small semi-field angle. When the thickness of the plane-parallel plate is taken into account, this method may be impractical.

(5) A trial to make a high-speed camera by extending the corrector plate is not successful.

Acknowledgement

The authors wish to express their gratitude to Professor T. Shimizu of Kyoto University for his valuable suggestions. Thanks are also due to Dr. Y. Watanabe, Chief of the Division of Applied Physics, Government Industrial Research Institute, and to Mr. K. Otani of the Institute who carried out a laborious work of plotting the final data of spot diagrams. One of the authors

(T.K.) wishes to express his thanks to Dr. B. Takase of Tokyo University, Dr. N. Matsunami of Tokyo Astronomical Observatory, Dr. T. Oki of Fukushima University and to the members of research group in the stellar astronomy in Japan.

REFERENCES

1) Carathéodory, C. : Hamburger Math. Einzelschriften, No. 28, 1940.
2) Lucy, F. A. : J. O. S. A., 30, 251-254, 1940.
3) Bowen, I. S. : Telescope, ed. by G. P. Kuiper & B. M. Middlehurst. *Stars and Stellar Systems*, Vol. I, Chap. 4, The Univ. of Chicago Press, 1960.
4) Linfoot, E. D. : Recent Advance in Optics. Chap. III, 176-183, Oxford Clarendon Pres, 1955.
5) Conrady, A. E. : Applied Optics and Optical Design, 2, 658-661, Dover Publ. Inc. New York, 1960.